

Development of CMOS Monolithic Active Pixel Sensors for the ALICE-ITS Outer Barrel and for the CBM-MVD

M. Deveaux*, D. Doering, B. Linnik, C. Müntz, J. Stroth

*Institut für Kernphysik, Goethe University Frankfurt,
Max-von-Laue-Str. 1, 60438 Frankfurt/M, Germany
E-mail: deveaux@physik.uni-frankfurt.de*

E. Spiriti

*Istituto Nazionale di Fisica Nucleare - Laboratori Nazionali di Frascati,
Frascati (Rome), Italy*

J. Baudot, G. Bertolone, A. Besson, G. Claus, C. Colledani, A. Dorokhov, G. Dozière, M. Goffe, A. Himmi, Ch. Hu-Guo, Q. Liu, F. Morel, A. Pérez Pérez, H. Pham, I. Valin, M. Winter

*IPHC, 23 rue du loess - BP28,
67037 Strasbourg cedex 2, France*

After more than a decade of R&D, CMOS Monolithic Active Pixel Sensors (MAPS or CPS) have proven to offer concrete answers to the demanding requirements of subatomic physics experiments. Their main advantages result from their low material budget, their very high granularity and their integrated signal processing circuitry, which allows coping with high particle rates. Moreover, they offer a valuable radiation tolerance and may be produced at low cost.

Sensors of the MIMOSA series have offered an opportunity for nuclear and particle physics experiments to address with improved sensitivity physics studies requiring an accurate reconstruction of short living and soft particles. One of their major applications is the STAR-PXL detector, which is the first vertex detector based on MAPS.

While this experiment is successfully taking data since two years, it was found that the 0.35 μ m CMOS technology used for this purpose is not suited for upcoming applications like the CBM micro-vertex detector (MVD) and the ALICE inner tracking system (ITS), which require faster and more radiation tolerant sensors. The exploration of a deeper submicron CMOS technology was therefore initiated. It was shown that MAPS can be envisaged for detectors exposed to running conditions significantly more severe than those of the STAR-PXL.

We report on major results obtained with this R&D and discuss our strategy toward the fabrication of sensors for the ALICE-ITS and the CBM-MVD.

*24th International Workshop on Vertex Detectors,
1-5 June 2015
Santa Fe, New Mexico, USA*

*Speaker.

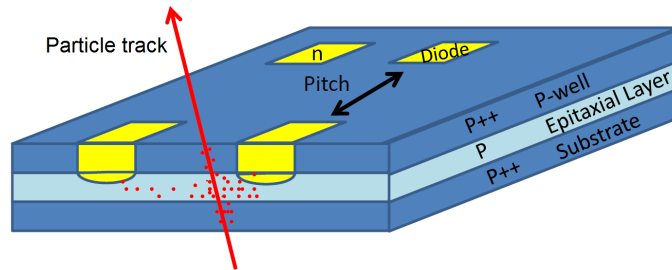


Figure 1: Simplified layout of the sensing elements of MAPS.

1. Introduction

CMOS Monolithic Active Pixel Sensors (MAPS or CPS) integrate sensing elements and digital and analogue signal processing circuitry on one single CMOS-chip. The active medium of their sensing elements are formed from a moderately P-doped epitaxial layer, which are found in various commercial CMOS wafers. As shown in Figure 1, this layer is located on top of the highly P-doped substrate of the wafer and below a layer formed from highly doped P-well implants. Impinging particles create electron-hole pairs in the epitaxial layer. In conventional CMOS-sensors, the epitaxial layer remains mostly undepleted and the electrons move by means of thermal diffusion. However, they are deflected by the build-in voltages of the P-epi/P++ interfaces between the epitaxial layer and the highly doped domains. Therefore, they are somewhat guided toward the N-well/P-epi diodes used for signal charge collection. Once they are collected, the electrons are stored in the parasitic capacity of the diodes and the related voltage drop is amplified by a dedicated low noise amplifier located in the pixel.

The strong points of MAPS used for charged particle detection are their very fine pixel pitch of a few $10\ \mu\text{m}$, which provides a high granularity and a few μm spatial resolution. Moreover, they may be thinned to $50\ \mu\text{m}$, which turns into an exceptionally light material budget. Both features are combined with an increasingly competitive readout speed and radiation tolerance.

The latter was initially limited to $\sim 10^{12}\ \text{n}_{\text{eq}}/\text{cm}^2$, as a consequence of the bulk damage reducing the life-time of the signal electrons in the epitaxial layer, which tend to recombine before reaching the collection diode. An improvement by about two orders of magnitude was reached once CMOS-processes with lowly doped (so-called high-resistivity) epitaxial layer became available. Their low doping increases the depletion depth of the collection diodes from a fraction of a μm to several μm , which dramatically accelerates the charge collection [1].

The readout speed of the sensors is mostly determined by the complexity of the on-chip data processing circuitry. Initially, only a pre-amplifier based on a source follower was integrated in each pixel. The pixel signal was multiplexed to a common, analogue readout bus and the data was processed and discriminated outside of the sensor [2]. For sensors with a sensitive area of a few centimetres squared, this concept allowed for frame readout times of some milliseconds. A substantial improvement was obtained by integrating the necessary analogue signal processing into the pixel amplifiers, grouping the pixels in columns and adding a discriminator to the end of each column. Accordingly, the slow, common, readout chain was replaced by ~ 1000 discriminator

	STAR-PXL	ITS (Outer)	ITS (Inner)	CBM (SIS100)
Spatial Resolution [μm]	< 4	< 10	< 5	< 5
Readout time [μs]	185.5	30	30	30
Ionizing Dose [krad]	150	100	2,700	3,000 ^(*)
Non-ionizing Dose [$n_{\text{eq}}/\text{cm}^2$]	3×10^{12}	1×10^{12}	1.7×10^{13}	3×10^{13} ^(*)
Operating Temperature [$^{\circ}\text{C}$]	35	30	30	-20
Power [mW/cm^2]	160	< 100	< 300	< 200
Area [m^2]	0.15	> 10	0.17	0.08
Bonding	Wedge	Laser	Laser	Wedge

Table 1: Design goals for the sensors of the STAR-PXL (already operational), the ALICE-ITS (outer layers), the ALICE-ITS (inner layers) and the CBM-MVD. (*) per year of operation.

chains operating in parallel and sending their digitised signals to an on-chip data sparsification circuit. This allowed for reducing the readout time to about 100 μs and preparing sensors for the STAR-PXL [3], which participates meanwhile to regular data taking campaigns of the experiment.

However, the performance reached is not sufficient for matching the more demanding requirements of the ALICE-ITS [4] and the CBM-MVD [5], which are listed in Table 1. In order to progress, it was decided to exploit the novel features provided by the Tower/Jazz 0.18 μm - CMOS process. This work will introduce the features of the process and point out its advantages as compared to elder 0.18 μm - CMOS processes. Hereafter, we discuss the current R&D strategy toward the sensors for ALICE and CBM and show current progresses of this R&D.

2. R&D toward a sensor for the outer barrel of the ALICE-ITS

2.1 R&D concept

The current R&D started from the MIMOSA-28 / ULTIMATE sensor, which is was successfully used to reconstruct D^0 -mesons within the STAR-experiment [6]. This sensor provides a column parallel readout and a high resistivity epitaxial layer as discussed in the previous section, its technical data is listed in Table 2. By comparing the performances of this sensor with the requirements of the experiments, one finds that the readout-time and the energy consumption of MIMOSA-28 are too high for using the sensor in the outer barrel of the ALICE-ITS. For CBM and the inner barrels of the ALICE-ITS, mostly the readout-time and the radiation tolerance are of concern.

To overcome those limits, it was decided to migrate the successful design to a novel 0.18 μm CMOS-process. As compared to the previously used 0.35 μm CMOS-process, the novel process features a higher integration density and intrinsic tolerance to ionizing radiation. Moreover, the presence of deep N- and P-wells allows the use of both, PMOS- and NMOS-transistors, within the pixel array. Finally, the foundry accepted to process customized wafers, provided they were guaranteed to fulfil a certain set of industrial norms.

Thanks to the novel features, it is possible to integrate a discriminator into the pixel itself and to go along with an asynchronous readout architecture inspired by the one used for hybrid pixels [8]. This feature is being exploited in the ALPIDE chip [9], which is currently considered as the most

	Mi-28	FSBB	Mi-22THR	MISTRAL-O ^(*)
CMOS process	0.35 μm	0.18 μm	0.18 μm	0.18 μm
Pixel (columns \times lines)	960 \times 928	416 \times 416	64 \times 64	832 \times 208
Pixel pitch [μm^2]	20.7 \times 20.7	22 \times 33	36 \times 62.5 39 \times 50.8	36 \times 65
Spatial Resolution [μm]	~ 4	~ 5	~ 10	~ 10
Readout time [μs]	185.6	41.6	~ 5	20.8
Ionizing Dose [krad]	> 150	> 1000 ^(**)	> 1000 ^(**)	> 150
Non-ionizing Dose [$n_{\text{eq}}/\text{cm}^2$]	> 3 $\times 10^{12}$	> 10 ¹³ ^(***)	$\sim 10^{13}$ ^(***)	> 10 ¹²
Power [mW/cm^2]	160	< 160	N/A	~ 80
Sensitive area [mm^2]	19.2 \times 19.9	13.7 \times 9.2	8 and 9 ^(IV)	13.5 \times 30.0
Bonding pads on pixel	No	No	Yes	Yes
On-chip cluster finding	1D	2D	None	2D

Table 2: Technical data and performances of the sensors discussed in this work. (*) Design goals. (**) Up to 10 Mrad according to preliminary results on simple pixels manufactured in the same technology [7]. (***) see text. (IV) depending on pitch.

promising approach for the inner layers of the ALICE-ITS. However, building and testing such a complex novel pixel structure comes with certain risks of fail and, more importantly, of project delays. Given the tight time line of the upgrade, it was decided to also build MISTRAL-O, a sensor dedicated to the sizeable outer layers of the ITS. This sensor is derived from the existing MIMOSA-28 and does not aim to reach the performances of ALPIDE. Instead, a focus is laid to provide a robust solution, expected to be intrinsically under reasonable control for a mass production.

As compared to MIMOSA-28, the readout speed of MISTRAL-O has to be accelerated by one order of magnitude while the dissipated power has to be reduced by a factor of about two. Additional challenges arise from the need to remain pin-to-pin compatible with ALPIDE, which introduces the need to integrate pads suited for laser bonding onto the pixel area. Moreover, the slow control and the digital logic of the sensor are to be adapted toward the ALICE/ALPIDE standards.

2.2 Status of the R&D

2.2.1 Validation of the readout chain of MISTRAL

A first step to migrate MIMOSA-28 to the novel 0.18 μm CMOS-process was made with the FSBB-M0 real scale prototype (technical data in Table 2). This sensor integrates the full analogue and digital readout chain of MIMOSA-28 but the readout time was boosted by a factor slightly above four. This was done by reducing the number of pixels in one column from 928 to 416 by i) reducing the length of the column and ii) increasing the size of the pixel along this column. Moreover, the readout of each column is now shared between two discriminators. Therefore, each discriminator has to read 208 instead of 928 pixels, which turns into a proportional speed-up of the readout process. The readout and slow control logic were not yet adapted to the ALICE-standard but its bandwidth was extended by a factor of four. Moreover, the internal cluster finder was

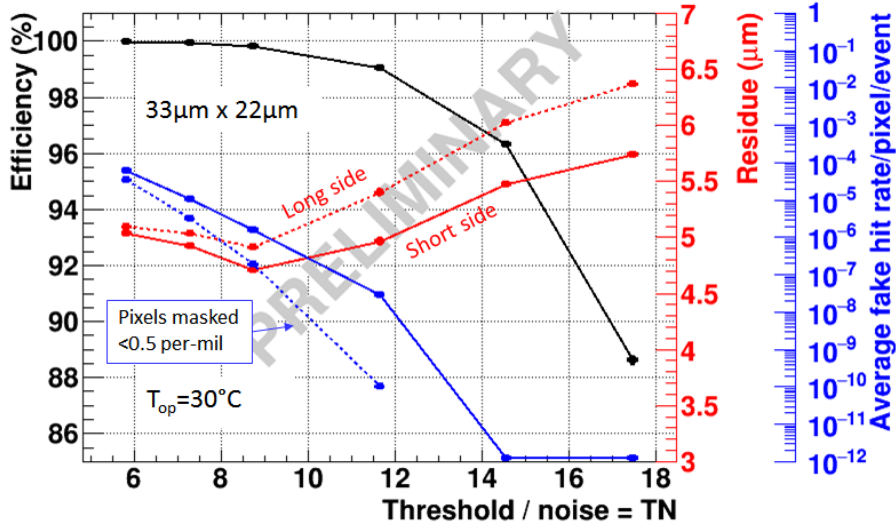


Figure 2: Detection efficiency, dark occupancy and spatial resolution of the FSBB sensor as a function of the discriminator threshold at an operating temperature of $T = 30^\circ\text{C}$. The threshold values are expressed in multiples of the pixel noise.

extended to identify 2-dimensional groups of pixels, while MIMOSA-28 identified hit clusters as multiple 1-dimensional groups, which had to be merged by external instances.

The sensor was tested in the laboratory and with a ~ 120 GeV/c negative particle beam at the CERN-SPS. Early results indicating a high pixel noise were caused by a minor bug in the layout of the digital circuitry of the sensor, originating cross coupling. The latter were mainly impacting the threshold scans performed for evaluating the noise components. During the beam test, the disturbance was significantly suppressed, since the pixels were operated in particle detection mode instead of threshold scan mode. As shown in figure 2, the measurements showed satisfactory results. A detection efficiency well above 99% in combination with a $< 10^{-5}$ dark occupancy was observed and the latter could be reduced by an order of magnitude by masking some (< 0.5 per-mil of all) pixels.

The spatial resolution of the FSBB was found to reach about $5 \mu\text{m}$. It is slightly higher along the long side than along the short side of the $22 \mu\text{m} \times 33 \mu\text{m}$ pixels. It is substantially better than one would expect for the digital readout implemented in the sensor according to the $1/\sqrt{12}$ -rule. This follows from the cluster pixel multiplicity, which is about 3 in average, thereby providing a spatial resolution based on the reconstruction of the centre-of-gravity of each pixel cluster. However, a subset of about 15% of all clusters show only one hit pixel. In principle, the spatial resolution of this subset cannot benefit from the centre-of-gravity reconstruction. The question was therefore addressed, on how worst the resolution of those clusters might be. The measurements show that clusters with a multiplicity of one exhibit in fact a resolution of better than $5 \mu\text{m}$ in both directions. They also show that such clusters are formed exclusively by particles impinging the pixel near the readout diode and such in the centre of the pixel. Alternatively, as soon as a particle hits the pixel array at some distance from the closest collection diode, its cluster includes systematically more than one pixel.

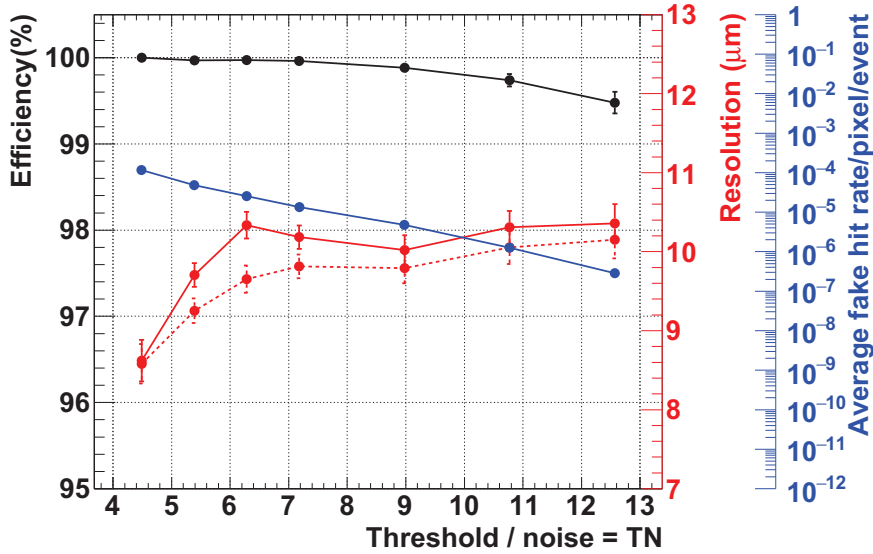


Figure 3: Detection efficiency, dark occupancy and spatial resolution of MIMOSA-22THR (b7) pixels with $39 \times 50.8 \mu\text{m}^2$ pitch as a function of the discriminator threshold at an operating temperature of $T = 30^\circ\text{C}$. The threshold values are expressed in multiples of the pixel noise.

2.2.2 Feasibility study on using pixels with $\sim 35 \times 65 \mu\text{m}^2$ large pixels

The above mentioned study on FSBB demonstrated successfully the migration of the MIMOSA-28 architecture to the $0.18 \mu\text{m}$ CMOS-process. To fully comply with the requirements of ALICE, the readout had to be accelerated by another factor of 1.5. Moreover, the power consumption of the sensor was to be reduced and the implementation of pads for laser bonding in the pixel array had to be validated. Those issues were addressed with the sensors MIMOSA-22THR (b5-b8). Like the previous generations of MIMOSA-22 prototypes [10], those test platforms host a pixel array, a full analogue readout chain including discriminators and slow control but (for the sake of cost and complexity reduction) no data sparsification circuitry.

The aim of reducing readout time and power was reached by increasing the size of the pixels to $36 \times 62.5 \mu\text{m}^2$ or $39 \times 50.8 \mu\text{m}^2$. This downscales once more the number of pixels per discriminator (generating the ambitious speed-up) and the number of columns per surface unit (reducing the number of discriminator chains needed and thereby the power consumption). As a drawback, one expected a loss of spatial resolution and tolerance to non-ionizing radiation, which were however foreseen to remain acceptable given the relaxed requirements in the outer layers of the ALICE-ITS (see Table 1). Moreover, the required pads for laser bonding were integrated on the top metal layers of the pixel array.

The MIMOSA-22THR prototypes were tested in the laboratory and with a $500 \text{ MeV}/c$ electron beam at LNF/BTF [11]. A representative result for a pixel with $39 \times 50.8 \mu\text{m}^2$ and a $4.8 \mu\text{m}^2$ diode cross-section is shown in figure 3. One observes that once more a detection efficiency substantially above 99% was reached in combination with a dark occupancy below 10^{-5} . This holds despite no pixels were masked during the test. The spatial resolution was found to be about $10 \mu\text{m}$ in both directions. Those excellent results do fully match the requirements for the outer layers of

the ALICE-ITS.

The tolerance of $33 \times 66 \mu\text{m}^2$ pixels to bulk damage was checked with pixels operating with analogue readout. The latter, which were hosted on a test structure called MIMOSA-34, were exposed to an integrated neutron flux of $10^{13} \text{ n}_{\text{eq}}/\text{cm}^2$. They were next operated at a temperature of 0°C and illuminated with the β -rays of a ^{90}Sr -source. The non-irradiated structure was observed to provide a most probable value of the signal over noise ratio (SNR) of 49, which decreased to 35 after irradiation. The study is not fully representative for MISTRAL-O, e.g. due to the lower operating temperature and due to the slightly higher depletion voltage. However, the radiation dose applied exceeds the requirements by one order of magnitude and the SNR remains a comfortable factor of two or three above the requirements for safe detector operation¹. Therefore, we don't expect the ongoing, more rigorous, radiation hardness studies to reveal negative surprises.

3. Summary, conclusion and Outlook

This paper summarises the latest outcome of an R&D on a CMOS Monolithic Active Pixel Sensor for the outer barrel of the ALICE-ITS. This sensor, MISTRAL-O, is based on the architecture of the MIMOSA-28 sensor, which is successfully operated in the STAR-PXL detector since 2014. To match the requirements of ALICE, the architecture was migrated to a $0.18 \mu\text{m}$ - CMOS process and the readout time is being reduced from $182 \mu\text{s}$ to $20.8 \mu\text{s}$ by i) reading two rows instead of one in parallel, ii) increasing the pixel size by about a factor of three along the column, iii) reducing the length of this column from 2.02 cm to 1.35 cm . Moreover, the enlarged pixel dimensions were chosen such as to provide sufficient power saving while keeping the spatial resolution $\lesssim 10 \mu\text{m}$ as required for the outer barrel.

The approach was validated with two complementary prototypes: FSBB featuring the complete signal generation and processing chain and MIMOSA-22THR featuring enlarged pixels with bonding pads on the pixel array. The FSBB-sensor allowed to validate the migration of the analogue readout chain of the sensor including the digital data sparsification circuits, though based on small ($22 \times 33 \mu\text{m}^2$) pixels. The feasibility to build sizeable ($36 \times 62.5 \mu\text{m}^2$ and $39 \times 50.8 \mu\text{m}^2$) pixels with bonding pads in the pixel area was demonstrated with the prototypes MIMOSA-22THR (b5-b8). Both chips were tested with particle beams and exhibited a detection efficiency well in excess of 99%, in combination with a dark occupancy below 10^{-5} , which matches the requirements.

Spatial resolutions of $\sim 5 \mu\text{m}$ and $\sim 10 \mu\text{m}$ were observed for pixels with $22 \times 33 \mu\text{m}^2$ and $39 \times 50.8 \mu\text{m}^2$ pitch, respectively. These values are below those expected from purely digital readout thanks to a centre-of-gravity analysis of the fired pixels composing a cluster. It was confirmed that the resolution does not degrade in case a particle hit features only one fired pixel.

A study based on other prototypes showed that large pixels with a pitch of $33 \times 66 \mu\text{m}^2$ tolerate $10^{13} \text{ n}_{\text{eq}}/\text{cm}^2$ according to their response to ^{55}Fe and ^{90}Sr -sources. Though the test remains to be repeated with the final sensor, this result is considered as strong evidence that the final sensor will tolerate the, by one order of magnitude lower, fluencies expected in the outer barrel of the ALICE-ITS.

¹According to our long lasting empirical experience, CMOS pixels show satisfactory performances during beam tests if their SNR for β -rays stays above 12 - 15.

We conclude that the requirements for the outer layers of the ALICE-ITS are matched in all aspects as far as the sensing elements, the analogue data processing circuits and the discrimination blocks are considered.

The next, and final, step will consist in manufacturing and test the complete sensor MISTRAL-O. The latter is designed to provide a sensitive area of $13.5 \times 29.95 \text{ mm}^2$, which will be covered with 832 columns made of 208 pixels each. The pixel dimensions will be $36 \times 65 \text{ }\mu\text{m}^2$, which turns into a $\sim 10 \text{ }\mu\text{m}$ spatial resolution and a $20.8 \text{ }\mu\text{s}$ readout time. The power dissipation will be $\sim 80 \text{ mW/cm}^2$. The digital readout will rely on building blocks similar to those of the ALPIDE sensor. It includes the option to receive up to six 80 Mbps data streams from neighbouring sensors and to multiplex them to one common 320 Mbps data link. This feature is to reduce the number of data buses on the readout cables and thereby to suppress their material budget.

Together with MISTRAL-O, 15 additional sensors will be submitted. Six among them will be used for studying well defined sensor parameters, which are suited to further optimize the performances of the pixel of MISTRAL-O. This study aims to gain additional tolerance to unexpected issues, as for example external sources of noise, and thereby to improve the robustness of the chip assembly. All sensors will be realized on various wafers with $18 - 30 \text{ }\mu\text{m}$ thick epitaxial layers with a doping corresponding to $1 - 8 \text{ k}\Omega \cdot \text{cm}$ resistivity. The best performing option will be chosen for the final sensor.

The first generation sensor for the CBM-MVD will be designed in a next step. It will presumably rely on the $22 \times 33 \text{ }\mu\text{m}^2$ -pixels mentioned above, which are expected to tolerate the additional radiation dose due to their smaller pitch and the lower operating temperature. Moreover, as already realized in FSBB, two 320 Mbps data links per cm^2 will be exploited to handle the substantially higher data rates of the CBM experiment.

Acknowledgements

This work was supported by HIC for FAIR, the German Ministry for Research and Education (BMBF, 05P12RFFC7) and the European Union (HP3-WP26). We thank our colleagues Cristina Bedda and Ivan Ravasenga from INFN Torino, and Paola La Rocca and Francesco Riggi from INFN Catania, for their contributions to the beam test of MIMOSA-22THR at INFN-LNF/BTF.

References

- [1] D. Doering et al., *Pitch dependence of the tolerance of CMOS monolithic active pixel sensors to non-ionizing radiation*, NIM-A Volume 730, 1 December 2013, Pages 111-114.
- [2] M. Szelezniak et al., *CMOS pixel vertex detector for STAR*, PoS(Vertex 2008)032.
- [3] J. Schambach et al., *A MAPS Based Micro-Vertex Detector for the STAR Experiment*, Physics Procedia 66 (2015) 514-519, and references therein.
- [4] B. Abelev et al. (The ALICE Collaboration), *Technical Design Report for the Upgrade of the ALICE Inner Tracking System*, 2014 J. Phys. G: Nucl. Part. Phys. 41 087002
doi:10.1088/0954-3899/41/8/087002.
- [5] M. Deveaux, J. Heuser for the CBM Collaboration, *The silicon detector systems of the Compressed Baryonic Matter experiment*, POS(Vertex 2013) 009 and references therein.

- [6] G. Van Buren, these proceedings.
- [7] D Doering et al., *Noise performance and ionizing radiation tolerance of CMOS Monolithic Active Pixel Sensors using a 0.18 μ m CMOS process*, 2014 JINST 9 C05051
doi:10.1088/1748-0221/9/05/C05051.
- [8] M. Garcia-Sciveres et al., *The FE-I4 pixel readout integrated circuit*, NIM-A Volume 636, Issue 1, Supplement, 21 April 2011, Pages S155-S159 and references therein.
- [9] M. Kofarago, these proceedings.
- [10] C. Hu-Guo et al., *Design and characterisation of a fast architecture providing zero suppressed digital output integrated in a high resolution CMOS pixel sensor for the STAR vertex detector and the EUDET beam telescope*, TWEPP, Naxos, Greece, September 2008, CERN-2008-008.
- [11] B. Buonomo, G. Mazzitelli and P. Valente, *Performance and upgrade of the DAFNE Beam Test Facility (BTF)*, IEEE Trans. Nucl. Sci. **52** (2005) 824.